OSCILLATORY FLOW ACROSS PLATES WITH DIFFERENT SHAPE OF EDGES

C. Weiyang[1] and F. A. Z. Mohd Saat[1,2*]

[1] Faculty of Mechanical Engineering, Universiti Teknikal Malaysia Melaka, Hang Tuah Jaya, 76100 Durian Tunggal, Melaka, Malaysia.

[2] Centre for Advanced Research on Energy, Universiti Teknikal Malaysia Melaka, Hang Tuah Jaya, 76100 Durian Tunggal, Melaka, Malaysia.

ABSTRACT

Oscillatory flow is the type of flow found in the greener thermoacoustic based technologies. Understanding the behavior of the less understood oscillatory flow of this kind is one of the key feature for the success of the system. Heat exchanger is one of the important part of the system. In this study, oscillatory flow across pile of hot and cold parallel-plates heat exchanger with three different shape of edges (i.e. rectangular, round and triangular shape of edges) were investigated. A suitable computational model was created in ANSYS. The results were compared to theoretical predictions and a good match was found. The study shows that the shape of the edge affects the flow and heat transfer of the system. A triangle-shaped edges with shorter length provides the higher heat transfer between plates and the oscillating fluid compared to plates with round and square edges. The results indicated that the entrance effect could be the reason for the change of heat transfer performance as the shape of edge changes.

KEYWORDS: *Oscillatory flow; Thermoacoustics; Heat exchanger; CFD.*

1.0 INTRODUCTION

Oscillatory flow is a cyclic flow found in engineering applications such as reactor and thermoacoustic systems. Thermoacoustic has been introduced into the industries for centuries. It can convert heat energy to work using thermoacoustic principles. Thermoacoustic, as the name goes, uses the combination of thermodynamics and acoustic as the working principle. It involves transfer of heat and also acoustical wave's movement. Besides, thermoacoustic also involves density and pressure variations in the production of energy process.

Nicholas Rott is the pioneer in deriving the correct equations for motion, pressure and time-averaged in energy transport in a channel with small, sinusoidal oscillations and with a temperature gradient (Swift, 2001). This eases the trouble of acoustic study on oscillations encountered in engines and refrigerators. Stirling engine century ago compromises a lot moving parts. In 1969, William Beale realized that under proper circumstances, forces on connecting rods will be small resulting in free-piston.

*Corresponding author e-mail: fatimah@utem.edu.my

Peter Ceperly, after realizing that time phasing between pressure and velocity in the thermodynamic elements of Stirling engine is the same as in acoustic travelling wave, suggested on removing every moving part except for the working gas itself. Not long after that, the Los Alamos group started their research and development of standing-wave thermoacoustic engines and refrigerators with different time phasing from Ceperly's idea and Stirling engine (Swift, 2001).

A thermoacoustic device can work in two ways. One is to produce work using heat and is mainly called as prime mover. Another way is to create heat by using work and is commonly called as heat pump. Thermoacoustic devices have gained more attention mainly due to its independence on moving parts and hence, more efficient. Furthermore it can be powered easily with sources such as solar or waste heat and the working medium is of environmental-friendly type. Last but not least, the cost of fabrication of such device is low and yet it is reliable (Piccolo, 2011). These are just few of the reasons why thermoacoustic devices are favorable nowadays.

The oscillatory flow conditions modelled in the current study will mimic the conditions found in thermoacoustic systems. The main working medium behind thermoacoustics is a type of flow called oscillatory flow. This flow is formed from sound waves with amplitudes high enough to transfer heat from one place to another. On the other hand, sufficient high temperature gradient can also create sound waves of reasonably high amplitudes. This principle plays an important role because the oscillatory flow will move back and forth expanding and contracting in order to do work.

2.0 LITERATURE REVIEW

Over the years, numerous researches had been carried out in the field of thermoacoustics. The type of fluid flow involved in thermoacoustic device is oscillatory flow where the fluid flow travels back and forth. Oscillatory flow can enhance heat transfer of a system. This has been proved experimentally and theoretically by Volk (2006). This feature is preferable in application such as a prime mover because heat is required to be dispersed as fast as possible in order to sustain the effectiveness of the prime mover. Heat transfer at the parallel-plates heat exchanger of a thermoacoustic system is very important as it will affect performance and efficiency of the device.

A simple explanation about devices using thermoacoustics principle may be explained with the aid of Figure 1. Generally the thermoacoustic effects occur within an area inside the device where structures shown in Figure 1 are placed. The structures, in general, contain a pile of solid structure known as 'stack'. This 'stack' is sandwiched between a pair of heat exchangers. Thermoacoustic effects occur when the oscillatory flow inside the device interacts with the 'stack'. Depending on the source of energy, the interaction between the flowing fluid and the solid surface of the stack may produce either cooling effect or power (Swift, 2001).

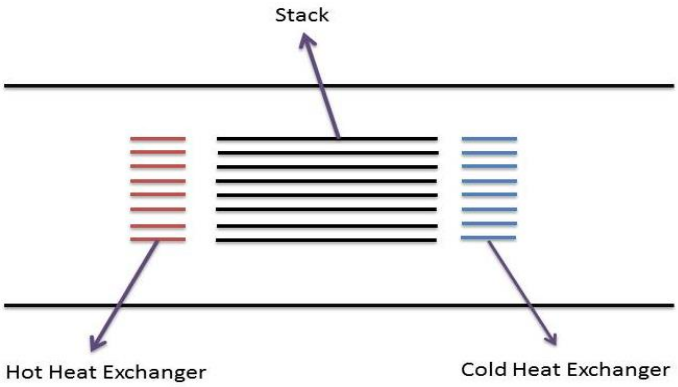

Figure 1. Illustration on position of heat exchangers and stack

The heat exchangers at the ends of 'stack' are responsible to effectively remove heat from the system and provide cooling capacity to the refrigerated space that is attached to the system. On the other hand, if the heat exchangers provide a high enough temperature gradient to the fluid, such that allows the fluid particle to excite, power will be produced. The energy produced may then be harnessed for other useful application (Swift, 2001).

The challenge in commercializing the thermoacoustic technologies lies, among others, on understanding the behavior of the flow and heat transfer phenomena inside the system. Current analytical solution used in designing the thermoacoustic system is based on a one-dimensional linear model. However, in practical system, the flow may consist of irregularities such as natural convection (Mohd Saat et al., 2012), streaming and vorticity (Mao et al., 2008). It is pertinent that these effects are investigated so that a proper understanding may be gained. This involves the fundamental knowledge of oscillatory flow. The study on heat transfer phenomenon in a heat exchanger across oscillatory flow is important. There are many types of heat exchanger and the parallel-plate heat exchanger is one of them. As the geometry of the parallel-plates structure is changed, the flow properties near the plates will also change (Irwan Shah et al., 2011). This may somehow affect the interactions between the oscillatory flow and the solid surfaces. The changing of geometry and the channel dimensions may also create disturbances or other effects on the flow. The usual shape of the plates is rectangle with sharp edges but what changes may be observed if the shape of the plates is changed for example, to rectangle with blunt edges or to other shape?

Whenever there is flow passing a solid body, a flow pattern such as vortices will be generated. Vortex is a mass of fluid or air moving in circular motion due to pressure changes. The center of vortex will commonly cause suction to the area around the vortex. Von Karman is a type of vortex shedding where detached pairs of vortex appear at the back of a bluff body alternately. Alternating vortex shedding has been the main cause for the failure of numerous designs. In a study regarding the vortex shedding flow patterns, it is said that oscillatory flows past bluff bodies usually gives a more complicated flow pattern than the Von Karman type of shedding in steady flows.

This is due to the oscillation of the flow that will cause impingement of vertices on the body and the interaction with vertices that are generated by the flow when the direction of flow is reversed (Shi et al., 2010). In another research, it has been shown that the flow pattern of oscillatory flow is more complex compared to those of steady flow. Therefore, the knowledge on the flow pattern around the structure of parallel plates is essential so that researchers can have clearer idea of the thermoacoustic effect at the structure such as stack or heat exchanger (Mao & Jaworski, 2010).

However, if the geometry of parallel plates and channel dimensions are changed, it may cause changes in the flow behaviors such as the boundary layer, viscous and thermal penetration depth and also the occurrence of vortex shedding. Boundary layer, a region of flow around the surface of parallel plates that may encounter viscous force, may bring disturbance to the heat transfer process between the flow and the solid boundaries. Difference in the gap dimension will cause the flow behaviors that are affected by thermal and viscous penetration depth to be disrupted. If the gap is too large, the thermal interaction between the flow and the solid boundaries may be too weak. In a study of geometrical optimization of thermoacoustic heat engines, it is shown by simulation that by decreasing the stack spacing, all the gas parcels are confined within the thermal boundary layer. This allows the gas parcels to interact with the stack and eventually increases the performance of the heat engine. However, if the stack spacing is decreased, the effect of viscous forces becomes greater causing rise in the viscous losses. Unfortunately, this will lower the performance of the heat engine. Therefore, the stack spacing needs to be maintained at an optimum level where the thermal effect is good whereas the viscous effect is not too strong (Ibrahim et al., 2011). Apart from that, the occurrence of vortex shedding at region around the parallel-plates has gained attention from researchers too. Few studies have been carried out to determine the effect of geometry on the formation of vortices around the stack in thermoacoustic devices. The application of oscillatory flow as working medium does not lighten the burden of researchers. Instead, the oscillatory flow along with the changes in cross section make the flow structures at the end of the stack even more complex (Mao et al., 2008). A deeper understanding of the flow throughout the internal structures of the system is necessary in order to design a high performance thermoacoustic heat engine. As the flow moves to the end of a rectangular plate with sharp edges, flow separation can be observed (Mao et al., 2008). When the flow is out of the channel, it may generate vortex-like wake which will complicate the flow pattern. Generation of vortices at the entrance and exit of the channel will cause the flow energy to dissipate into heat and therefore reducing the performance of the thermoacoustic device.

In this study, a flow pass a pile of parallel-plates acting as heat exchangers will be modelled. The fluid will flow back and forth in an oscillatory manner. There will be formation of various flow patterns when a fluid flows past the parallel-plates. Besides, there is also heat transfer between the two entities since the parallel-plates will be acting as heat exchangers. The temperature difference around the plates region will cause the occurrence of heat transfer between the fluid and the plates due to the temperature gradient. The focus of this investigation is to study how the changes in the plate geometry (shape of edges of the parallel-plate) may disturb or affect the flow and heat transfer across a parallel-plate heat exchanger.

3.0 COMPUTATIONAL MODELLING

The domain used in this study is a simplified model for parallel-plates heat exchangers. The dimensions of the domain are set in accordance to Mohd Saat and Jaworski (2013) in order to facilitate the validation of the model. The length of the horizontal walls is set to be 600 mm while the height is set to be 132 mm. The total length of the parallel-plate structure is 70 mm. Hot heat exchanger is represented by half of the length of the parallel-plate, that is 35 mm. The other half of the parallel-plate represents cold heat exchanger. The parallel-plates have thickness of 3.2 mm with 6 mm wide gap between the plates. The pile of parallel-plates is located at 265 mm from the inlet and 23 mm from the bottom wall. There are a total of 10 plates in parallel arrangement. The side of parallel-plates in red represents the hot heat exchanger while the side in blue represents cold heat exchanger.

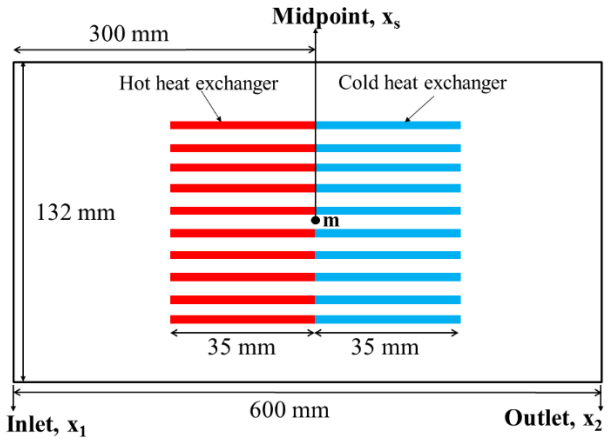

Figure 2. Illustration of the computational domain and its dimensions

The model was solved using a pressure-based solver. A transient solver was selected to model the cyclic nature of the oscillatory flow. The effect of gravity was also turned on to correctly model natural convection due to the presence of the hot plate. Taking upwards direction as positive, acceleration in y-direction was set to be -9.81 m/s^2 which is the gravity acceleration. Heat transfer was modelled using two-dimensional energy equation with the consideration of viscous dissipation. This is to ensure that heat transfer process within the plates and nearby areas are modelled correctly. For the pressure-velocity coupling, SIMPLE algorithm was chosen. Nitrogen gas was selected as the working medium of the domain. The gas was modelled as compressible flow. The thermal conductivity of the gas was set as temperature-dependent following the equation proposed by Abramenko et al., (1992). The boundary conditions of the computational domain were calculated using lossless equation as shown in Equations (1) and (2) (Mohd Saat & Jaworski, 2013).

$$P_1 = P_a \cos(k_a x_1) \cos(2\pi f t) \quad (1)$$

$$m_1 = (P_a/c) \sin(k_a x_2) \cos(2\pi f t + \theta) \quad (2)$$

The term P_a is pressure at pressure antinode, ka is wave number and c is the speed of sound with a value of 353 m/s. The value of x_1 is 4.23 m and x_2 is 4.83 m.

The flow amplitude modelled in this study is for the drive ratio of 0.3%. The drive ratio is defined as the ratio between pressure at antinode and the mean pressure. The mean pressure was set as atmospheric pressure. The wave number, k_a, was calculated as $2\pi/\lambda$, where $\lambda=c/f$ is the wavelength. The frequency, f, of the flow was set to be 13.1 Hz. The phase, θ, between outlet mass flux, m_1, and the inlet pressure was set to 90° so that the flow is in standing wave mode. The simulation was run for a minimum of 40 cycles so that the simulation reached a steady oscillatory flow condition.

Figure 3 shows the sketch of the parallel-plate heat exchanger used in this study. The original model has a rectangular shape of edge. Case 1 has a round shape of edge, while Cases 2 and 3 have a rectangular shape of edges. However the rectangular shape of edges in Cases 2 and 3 are different in sizes. Case 3 has the longest horizontal distance because the distance from the original edge to the tip of triangle is two times of that for Case 1 and Case 2. Note that the total length of all the four cases investigated are slightly different. However, the total area of hot and cold plates (for the calculation of heat) four all the four cases are the same. The mesh numbers and sizes for these three cases were adjusted so that suitable meshing can be acquired. The configurations for solver settings for these three cases are the same as the configurations used for the original model.

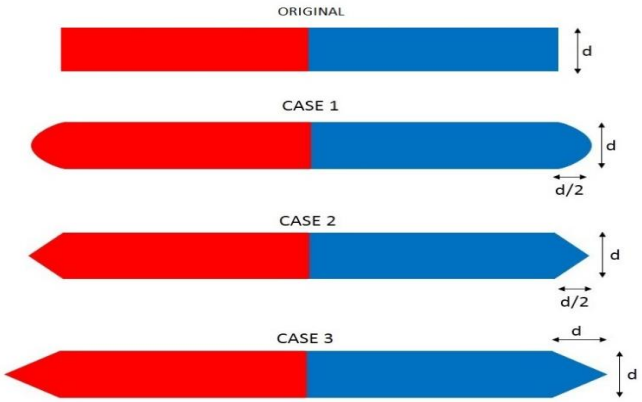

Figure 3. Geometry of simulation models with different geometries

4.0 MODEL VERIFICATION

The model was verified by comparing the axial velocity changes over time at point ‘m’ (please refer to Figure 2 for the location of ‘m’) between the results from simulation and the results from theoretical calculation using Linear thermoacoustic model as reported in Swift (2001). The velocity magnitudes of this oscillatory flow were recorded for 20 phases within one flow cycle. Figure 4 shows that the velocity increases from phases 1 to 5 and then decreases as it flows until phase 10. The fluid starts reversing after phase 10 with an increase of reverse velocity magnitude until phase 15. After that, the velocity of the reverse flow decreases and the flow will repeat with a new cycle after phase 20. As shown in Figure 4, a good match was found between the results and the theoretical predictions.

A closer look will reveal that the simulation results differ slightly from theory particularly between phases 4 to 10. The maximum percentage of error between the theory and results from simulation was determined to be 2.48% which is still acceptable. Thus, this simulation model was considered acceptable and can be used for simulation of the other models with different plate geometries.

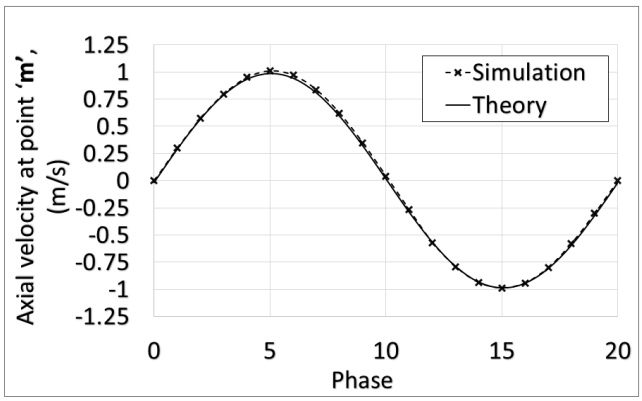

Figure 4. Changes of x-velocity of point '**m**' at different phases

Figure 5 shows the grid sensitivity test for this study where the simulation was run using another model with higher number of meshes. It can be seen that with higher number of meshes, deviation occurs between phases 4 to 12. The greatest deviation occurs at phase 9 with a percentage error of 8 percent. This indicates that with different number of meshes, the results obtained from this study may slightly differ. However, the model with the most appropriate number of meshes was already selected for this study so that the curve obtained will be similar to that predicted by theoretical calculation.

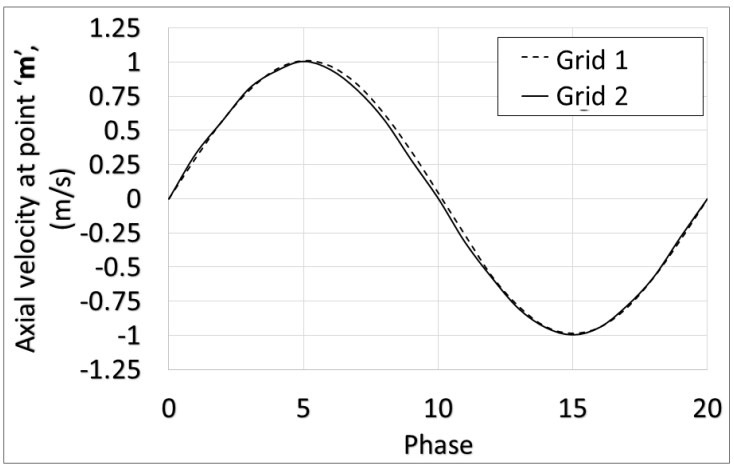

Figure 5. Grid sensitivity test

5.0 RESULTS AND DISCUSSIONS

5.1 Comparison of vorticity contours near the edges

Figure 6 shows that the vortex pair formed at the end of plate for Cases 2 and 3 are more symmetry compared to the other two cases. This indicates that flow is less disturbed at the end of plate when the edge is made in triangular shape. The existence of two layers of vorticity adjacent to the wall within the channel indicates that rotational flow occurs near the plate. This is a typical phenomenon for oscillatory flow where fluid flows back and forth in a cyclic manner. At phase 10, the flow is about to reverse. This explains the existence of the two layers of vorticity with different signs at locations near the wall. In overall, the strength of the second layer of vorticity away from the wall is stronger for Cases 1, 2 and 3. The flow was able to enter the channel smoothly for the three different shape of edges for Cases 1, 2 and 3. Thus, the stream of vortices for all the models other than the original model flew smoothly into the channel at phase 10. However for the original model, the second layer of vorticity is weak. This indicates that the flow was slightly disturbed hence showing signs of vortices discontinuities when the flow was heading into the channel from the right side.

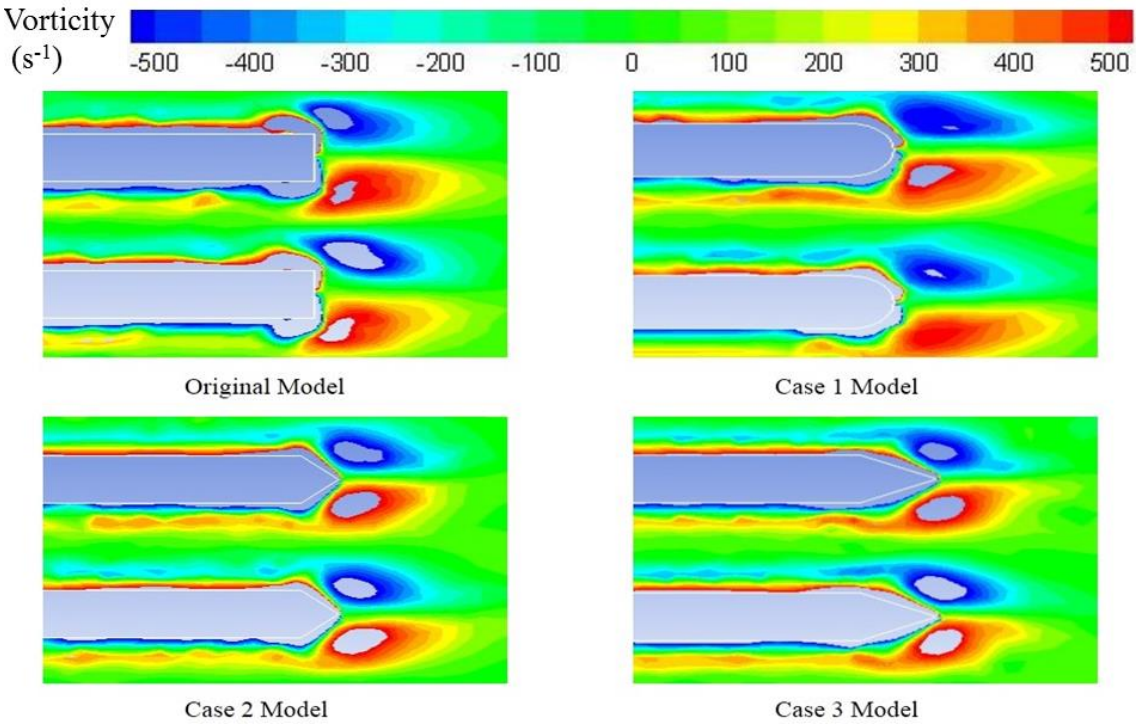

Figure 6. Vorticity contours near the edges of all the models at phase 10

Unfortunately, for 0.3 percent drive ratio the flow tend to be laminar. Hence the differences in shape of vortices at the edges between the models cannot be seen clearly. If the models were to be simulated with turbulent flow, such as at higher drive ratio, the differences could be clearer and easier to be observed.

5.2 Comparison of average total surface heat flux between all cases

The effect of edge shape on the heat transfer performance of the parallel-plate heat exchanger is examined by looking at the total surface heat flux gained at the heat exchanger's plate. Heat flux at the surface is defined as:

$$q = -k\frac{dT}{dy} \tag{3}$$

The terms q, k, T and y are the heat flux, thermal conductivity of the gas medium, temperature and vertical distance from the surface of the plate, respectively. The total surface heat flux for all cases presented in Figure 7 was calculated based on an area-weighted average of the heat which was also averaged over one flow cycle.

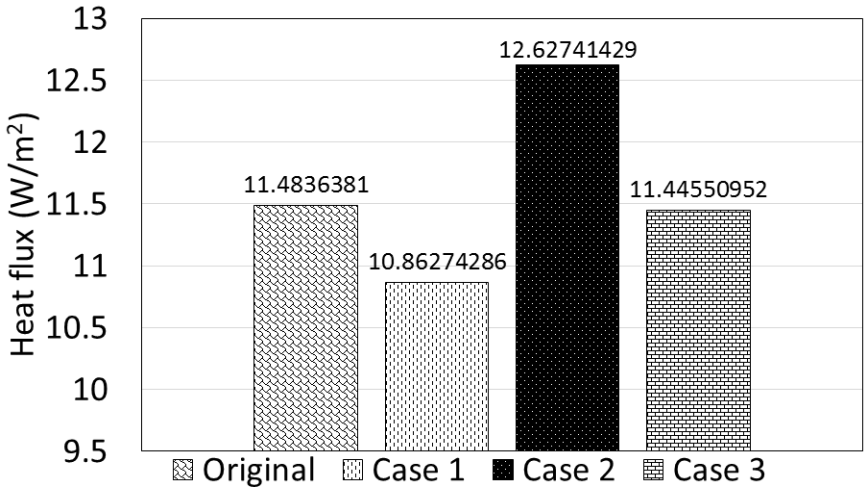

Figure 7. Average total surface heat flux at hot heat exchangers for all cases

It is clearly shown in Figure 7 that Case 2 has the highest average total surface heat flux over time at the hot heat exchangers surfaces compared to the other 3 cases. With reference to Figure 3, Case 2 was defined as the parallel-plate structure with a triangular shape of edge. Case 2 recorded a value of 12.6274 W/m^2 while the lowest value of average total surface heat flux recorded is from Case 1 with only 10.8627 W/m^2. The original model and Case 3 have almost the same value with original model being slightly higher than Case 3. The heat energy transfer rate at hot heat exchangers surfaces for Case 2 has shown huge increment after the alteration in the geometries of the edge of the parallel-plates. This is probably due to the change of flow structure within the layer which enhances the heat transfer at the plate.

5.3 Comparison of total surface heat flux between all cases

Detail analysis could be done by looking at the local heat flux values at several locations from the entrance of the left end of the parallel-plate structures as illustrated in Figure 8. As shown in Figure 8, the location for points 'A', 'B' and 'C' are 270 mm, 280 mm and 290 mm respectively from the left end of the computational domain.

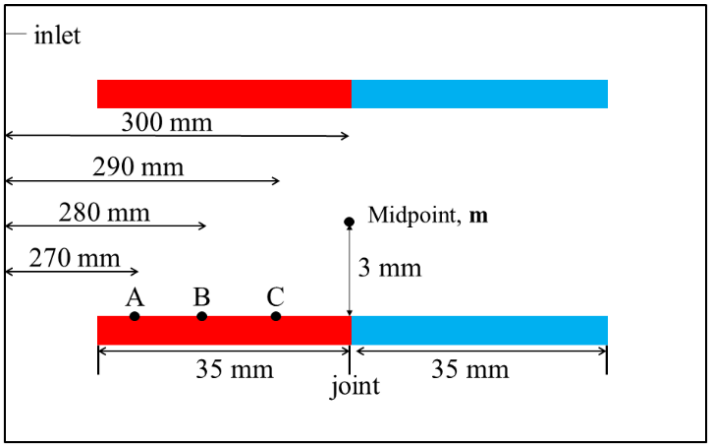

Figure 8. Location of point 'A', 'B' and 'C'

Note that the illustration in Figure 8 is represented using an enlarged view of just one pair of parallel-plate structures. The total number of plates in the real domain was as reported in Figure 2. The locations of points 'A', 'B' and 'C' are the same for all the models and the points are located on the hot heat exchanger side. Figure 9 shows the variation of local heat flux measured at location 'A' over twenty phases within one flow cycle. Location 'A' is located near the left entrance and far from the joint between the hot and cold plates. Case 2 which has a triangle-shaped edges with shorter edge length has the highest local surface heat flux at point 'A' for most of the phases. This could be related to the change of entry length due to the change of edge's shape. Mohammed and Salman (2007) proposed in their experimental study that as the entrance section length becomes longer, heat transfer decreases. This is probably caused by the resistance exerted from the flow as the entry length increases. Based on this argument, Case 2 with the highest value of local surface heat flux seems to have the shortest entry length presumably due to the less flow disturbance at the edge. As mentioned earlier, flow across original model seems disrupted particularly at the edges because of the rectangular shape of the edges. The triangle shape of edge has smaller form drag compared to rectangle shape of edge. Hence, the triangle shape of edge of Case 2 provides a smoother path for the fluid to oscillate. As a result, a better heat transfer through point 'A' is possible. However, if the triangle edge is made longer (Case 3) the heat flux drops. The results shown in Figure 9 also shows that the heat flux values for round edge (Case 1) are also consistently smaller than Case 2 and original model. The reason for this is not clear but could be related to the effect of the viscous and thermal boundary layers which may change as the fluid flow through the edge with different shape. Furthermore, the performance of heat transfer can also be greatly affected by vortices (Shi et.al., 2010). A deeper study in this area may be needed to help understand this phenomena.

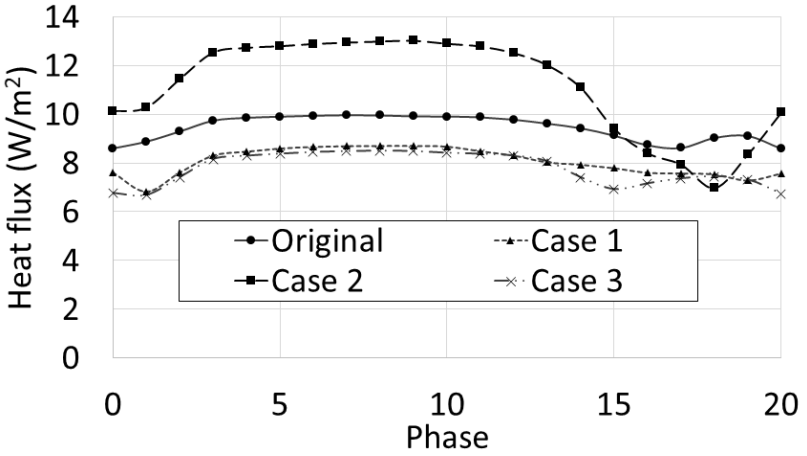

Figure 9. Local surface heat flux at point 'A' for all the cases

Figure 10 shows the local heat flux at location 'B'. Location 'B' is located somewhere midway between the left entrance and the joint between the cold and hot plates. It is noteworthy that the temperature gradient at the joint between the cold and hot plates is very high. Since point 'B' is located midway between the left end and the joint, the thermal and viscous layer at this point are expected to be less affected by the entrance effect and the effect of temperature gradient at the joint. This effect could be seen in the original model, Case 2 and Case 3 which have recorded only slight fluctuations of local surface heat flux throughout the phases. However, Case 1 showed significant fluctuations of values for local surface heat flux at point 'B'. Case 1 which has round-shaped edges also has the highest value of local surface heat flux at almost all phases. This indicates that the viscous and thermal layer of Case 1 are not as steady as the other three cases even at locations away from the entrance and the joint.

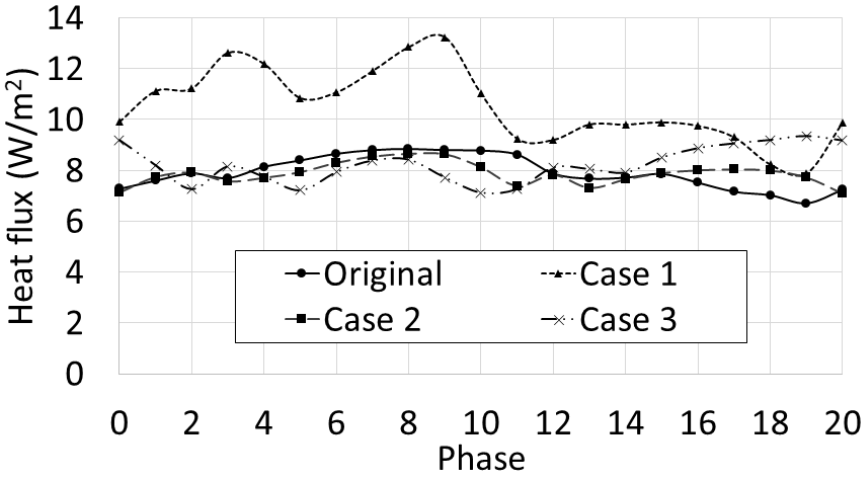

Figure 10. Local surface heat flux at point 'B' for all the cases

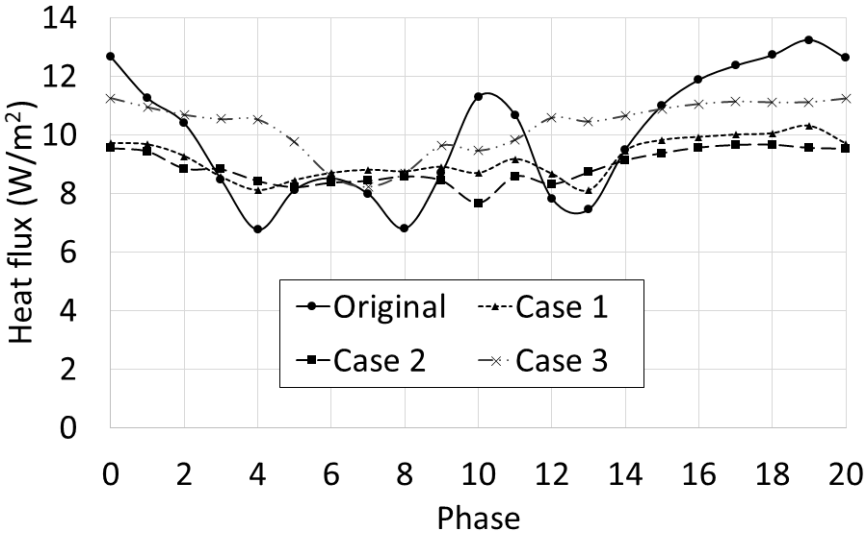

Figure 11. Local surface heat flux at point 'C' for all the cases

Figure 11 shows the local heat flux at location 'C'. Location 'C' is located near the joint where temperature different between the hot and cold plates is high. According to Figure 11, both Case 1 and Case 2 showed similar results. The curves for both cases are almost similar for all the phases. Local surface heat flux at point 'C' for Case 3 also showed minor fluctuations throughout the phases. This fluctuations are very small. The original model, however, showed huge fluctuation of values of local surface heat flux through the entire phases. The curve for original model showed uphill and downhill trend several times. This indicates that the original model felt the effect of the temperature gradient the most. The rectangular-shaped edge alters the condition of flow at this point so that the temperature gradient at the joint has the greatest influence on heat transfer at point 'C'. The results presented in Figures 10 to 11 indicate that the high value of total heat flux for Case 2, as presented in Figure 7 may be due to the influence of entrance length. This is based on the high value of heat flux for Case 2 at location 'A' as presented in Figure 9. Other fluctuations of local heat flux value at points 'B' and 'C' seem to have minor effect on the total heat flux.

5.4 Comparison of average totral surface heat flux between all cases

Velocity profile near the entrance at point 'A' (refer Figure 8 for point 'A') is compared between all the cases. A vertical line was created from point 'A' to the bottom surface of the parallel-plates above point 'A'. The line connects the two parallel-plates and axial velocity data can be extracted through the line. The data were extracted at phase 5 where the fluid flows forward at maximum velocity and phase 15 where the maximum velocity of the reverse flow is achieved. The size of gap between the parallel plates is 6 mm. Therefore the value of 0.006 m in Figure 12a and Figure 12b is the distance from point 'A' to the bottom surface of the parallel-plates heat exchanger above it.

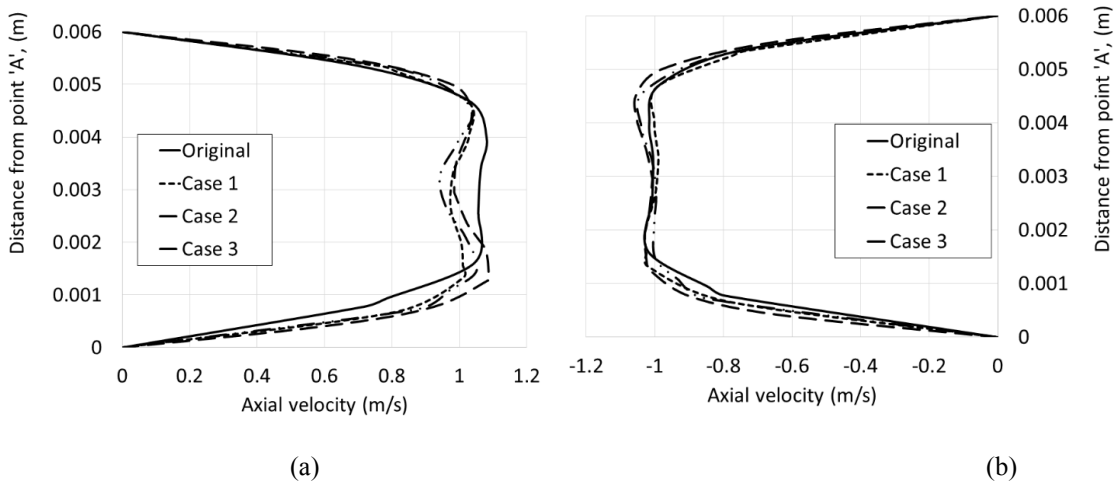

Figure 12. Velocity profile for all the cases at location 'A' for (a) phase 5 and (b) phase 15

Figure 12 shows the velocity profiles for all the cases at phases 5 and 15 when the flow is at the highest value of magnitude during the first half and second half of the cycles, respectively. The velocity profile at phases 5 and 15 for original case is symmetry. They have a form closest to the fully developed flow profile. All other cases presented asymmetry velocity profiles between the two stages of the flow cycle. At phase 5, the velocity boundary layers of the other 3 cases seem not yet reaching the fully developed profile. These behaviors may be related to the entrance effect. However when the flow reversed its direction at phase 15, the velocity profile for most of the cases are similar and the profiles are more fully-developed like. When the flow reversed its direction, it entered the channel from the cold heat exchanger sides. During this part of a flow cycle, the flow have already travelled for a certain distance before it reach point 'A'. Thus, the velocity boundary layer for all the cases have developed fully forming the fully-developed shape of velocity profile as seen in Figure 12 (b).

6.0 CONCLUSIONS

The flow and heat transfer of the validated original model were analyzed and compared to the results of the other three cases with different shape of plate edges. At the low drive ratio investigated in this study (0.3% drive ratio), the vortex structures at the end of the plate are slightly different from one case to another as the shape of edge changes. The difference is not so big due to the laminar feature of the low drive ratio investigated. As drive ratio increases the vortex pattern is expected to be more complicated. Future work should look into this matter closely. It is expected that the edge shape will give a more significant impact on the vortex pattern when fluid oscillates at higher drive ratio. The results also showed that the heat transfer performance may be different if the shape of edges are different. This study suggested that a triangle-shaped edges with shorter length provides the higher heat transfer between plates and the oscillating fluid. The results of the local heat transfer investigation and velocity profiles shown at point 'A' suggest that the increase of heat may be related to the entrance length which was altered due to the change of shape of edge. However, deeper investigations are needed so that a better understanding could be

gained about the viscous and thermal boundary layers influence on the flow and heat transfer of an oscillatory flow across the parallel-plate structures.

ACKNOWLEDGEMENTS

The authors would like to thank Universiti Teknikal Malaysia Melaka (UTeM) and Ministry of Education (MOE) Malaysia for supporting this research activities. This research work is part of the works funded by MOE under a grant FRGS/1/2015/TK03/UTEM/03/3.

REFERENCES

Abramenko T. N., Aleinikova V. I., Golovicher L. E., & Kuz'mina N. E. (1992). Generalization of experimental data on thermal conductivity of nitrogen, oxygen, and air at atmospheric pressure. *J. Eng. Thermophys*, *63*, 892-897.

Ibrahim, A. H., Arafa, N. M., & Khalil, E. E. (2011, January). Geometrical Optimization of Thermoacoustic Heat Engines. *Mechanical Power Engineering*.

Irwan Shah, A., Normah, M., Jamaluddin, M., Aminullah, A., & Dairobi, G. (2011). Stack Geometry Effects on Flow Pattern With Particle Image Velocimetry (PIV). *Jurnal Mekanikal 33*, 82–88/.

Mao, X., & Jaworski, A. J. (2010). Oscillatory flow at the end of parallel-plate stacks: phenomenological and similarity analysis. *Fluid Dynamics Research*, *42(5)*, 055504.

Mao, X., Yu, Z., Jaworski, A. J., & Marx, D. (2008). PIV studies of coherent structures generated at the end of a stack of parallel plates in a standing wave acoustic field. *Experiments in Fluids, 45(5)*, 833–846.

Mohammed & Salman (2007). The effects of different entrance sections length and heating on free and forced convective heat transfer inside a horizontal circular tube. *International Communications in Heat and Mass Transfer, 34(6)*, 769-784.

Mohd Saat, F. A. Z., & Jaworski, A. J. (2013, July). Oscillatory Flow and Heat Transfer Within Parallel-plate Heat Exchangers of Thermoacoustic Systems. *International Conference of Mechanical Engineers*, London, United Kingdom.

Mohd Saat, F.A.Z., Jaworski A.J., Mao X., & Yu Z. (2012, July). CFD modelling of flow and heat transfer within the parallel-plate heat exchanger in standing wave thermoacoustic system. In *Proceedings of the 19th International Congress on Sound and Vibration*, Vilnius, Lithuania.

Piccolo, A. (2011). Numerical computation for parallel plate thermoacoustic heat exchangers in standing wave oscillatory flow. *International Journal of Heat and Mass Transfer, 54 (21-22),* 4518–4530.

Shi, L., Yu, Z., & Jaworski, A.J. (2010). Vortex shedding flow patterns and their transitions in oscillatory flows past parallel-plate thermoacoustic stacks. *Experimental Thermal and Fluid Sciences, 34(7),* 954-965.

Swift, G. (2001). Thermoacoustics: *A unifying perspective for some engines and refrigerators. (Fifth Draf).* Los Alamos National Laboratory.

Volk, J. (2006). *Enhancing heat transport through oscillatory flows*. PhD thesis, University of Florida.